Journal of Statistical Physics, Vol. 99, Nos. 1/2, 2000

Nonequilibrium Phase Transition in a Model of Diffusion, Aggregation, and Fragmentation

Satya N. Majumdar,[1] Supriya Krishnamurthy,[2] and Mustansir Barma[1]

Received August 9, 1999; final October 18, 1999

We study the nonequilibrium phase transition in a model of aggregation of masses allowing for diffusion, aggregation on contact, and fragmentation. The model undergoes a dynamical phase transition in all dimensions. The steady-state mass distribution decays exponentially for large mass in one phase. In the other phase, the mass distribution decays as a power law accompanied, in addition, by the formation of an infinite aggregate. The model is solved exactly within a mean-field approximation which keeps track of the distribution of masses. In one dimension, by mapping to an equivalent lattice gas model, exact steady states are obtained in two extreme limits of the parameter space. Critical exponents and the phase diagram are obtained numerically in one dimension. We also study the time-dependent fluctuations in an equivalent interface model in $(1+1)$ dimension and compute the roughness exponent χ and the dynamical exponent z analytically in some limits and numerically otherwise. Two new fixed points of interface fluctuations in $(1+1)$ dimension are identified. We also generalize our model to include arbitrary fragmentation kernels and solve the steady states exactly for some special choices of these kernels via mappings to other solvable models of statistical mechanics.

KEY WORDS: Diffusion; aggregation; phase transition; nonequilibrium.

I. INTRODUCTION

By now, there is a fairly good understanding of the nature and properties of phase transitions in systems in thermal equilibrium, as one changes the

[1] Department of Theoretical Physics, Tata Institute of Fundamental Research, Mumbai 400005, India.

[2] Laboratoire Physique et Mécanique des Milieux Hétérogenes, École Supérieure de Physique et Chimie Industrielles, 75231 Paris Cedex 05, France.

0022-4715/00/0400-0001$18.00/0

strengths of external fields such as temperature, pressure or magnetic field. On the other hand there is a wide variety of inherently *nonequilibrium* systems in nature whose steady states are not described by the equilibrium Gibbs distribution, but are instead determined by the underlying microscopic dynamical processes. The steady states of such systems may undergo nonequilibrium phase transitions as one changes the rates of the underlying dynamical processes. As compared to their equilibrium counterparts, these nonequilibrium steady states and the transitions between them are much less understood owing to the lack of a general framework. It is therefore necessary to study simple models of nonequilibrium processes, both in order to discover new types of transitions as well as to understand the mechanisms which give rise to them.

In this paper, we study nonequilibrium phase transitions in an important class of systems which involve the microscopic processes of diffusion, aggregation upon contact and fragmentation of masses. These processes arise in a variety of physical settings, for example, in the formation of colloidal suspensions,[1] polymer gels,[2] river networks,[3,4] aerosols and clouds.[5] They also enter in an important way in surface growth phenomena involving island formation.[6] Below we introduce a simple lattice model incorporating these microscopic processes and study the nonequilibrium steady states and the transitions between them both analytically within mean field theory and numerically in one dimension. Some of the results of this paper have been reported earlier in a shorter version.[7]

The paper is organized as follows. In Section II, we define the model and summarize our main results. In Section III, we solve the mean field theory exactly and characterize the phases and the transitions between them. In Section IV, we report the results of numerical simulations in one dimension for both symmetric and asymmetric transport of masses. In Section V, the model in one dimension is mapped exactly to a lattice gas model whose properties are used to deduce the steady state mass distribution exactly in two extreme limits. In Section VI, we map this lattice gas model further to an interface model and make connections to other well studied interface models in some limits. We study the dynamics by computing the width of the interface both analytically in some limiting cases and numerically otherwise. We identify two new fixed points of interface dynamics in $(1+1)$ dimension. In Section VII, we generalize our model to include an arbitrary fragmentation kernel and obtain exact results for special choices of this kernel via mappings to other solvable models of statistical mechanics. In the Appendix we outline the exact solution for uniform fragmentation kernels. Finally we conclude with a summary and a discussion of a few open questions in Section VIII.

II. THE MODEL

Our model of diffusion, aggregation and dissociation is defined on a lattice, and evolves in continuous time. For simplicity we define it on a one-dimensional lattice with periodic boundary conditions although generalizations to higher dimensions are quite straightforward. Beginning with a state in which the masses are placed randomly, a site i is chosen at random. Then one of the following events can occur:

1. Diffusion and Aggregation: With rate p_1, the mass m_i at site i moves either to site $i-1$ or to site $i+1$. If it moves to a site which already has some particles, then the total mass just adds up; thus $m_i \to 0$ and $m_{i\pm1} \to m_{i\pm1} + m_i$.

2. Chipping (single-particle dissociation): With rate p_2, a bit of the mass at the site "chips" off, i.e., provided $m_i \geqslant 1$, a single particle leaves site i and moves with equal probability to one of the neighbouring sites $i-1$ and $i+1$; thus $m_i \to m_i - 1$ and $m_{i\pm1} \to m_{i\pm1} + 1$.

We rescale the time, $t \to p_1 t$, so that the diffusion and aggregation move occurs with rate 1 while chipping occurs with rate $w = p_2/p_1$.

This model clearly is a very simplified attempt to describe systems with aggregation and dissociation occuring in nature. For example, if one is thinking of gelation phenomena, then a polymer of size k is represented by a point particle of mass k in our model. Thus we ignore the spatial shape of the real polymer which however can play an important role under certain situations. We have also assumed that the fusion of masses after hopping or chipping occurs instantaneously, i.e., the reaction time scale is much smaller than the diffusion time scale. Thus our model is diffusion-limited. A somewhat more severe assumption is however that both desorption and diffusion rates are independent of the mass. In a more realistic situation these rates will depend upon the mass. However, our aim here is not to study any specific system in full generality, but rather to identify the mechanism of a dynamical phase transition, if any, in the simplest possible scenario involving these microscopic processes. If one is interested in a more realistic description of any specific system, one could and should include these features in the model. But for the purpose of this paper, we stay with the simplest version and show below that even within this simplest scenario, novel dynamical phase transitions occur which are non-trivial yet amenable to analysis.

In this model, the total mass M is conserved and fixed by the initial condition. Let $\rho = M/N$ denote the density, i.e., mass per site where N is number of sites of the lattice. In the above definition of the model, a mass at each site can move symmetrically either to the left or to the right with

equal probability. We call this the symmetric conserved-mass aggregation model (SCA). In this paper we also study the fully asymmetric version of the model where masses are constrained to move only in one direction (say to the left). We call this the asymmetric conserved-mass aggregation model (ACA). In the sections that follow, we show that the nonequilibrium critical behaviour of SCA and ACA belong to different universality classes. This can be traced to the fact that in the asymmetric case there is a nonzero mass current density in the system.

In both of these models, there are only two parameters, namely the conserved density ρ and the ratio $w = p_2/p_1$ of the rate of chipping of unit mass to that of hopping of the entire mass on a site, as a whole. The question that we mainly address in this paper is: given (ρ, w), does the system reach a steady state in the long time limit? If so, how can we characterize this steady state? We show below that indeed for all (ρ, w), the system does reach a steady state. This is a nonequilibrium steady state in the sense that for generic values of (ρ, w) it is not described by the Gibbs distribution associated with some Hamiltonian. In order to characterize the steady state we study the single site mass distribution function $P(m, t)$ as the time $t \to \infty$. We show below that there exists a critical curve in the (ρ, w) plane across which the steady state behaviour of the system, as characterized by $P(m)$, undergoes a novel phase transition.

Let us summarize our main results: In our model, there are two competing dynamical processes. The diffusion cum coalescence move tends to produce massive aggregates at the expense of smaller masses, and in this process, also creates more vacant sites. The chipping of single units of mass, on the other hand, leads to a replenishment of the lower end of the mass spectrum. The result of this competition is that two types of steady states are possible, and there is a dynamical phase transition between the two across a critical line $\rho_c(w)$ in the (ρ, w) plane. For a fixed w, if $\rho < \rho_c(w)$, the steady state mass distribution $P(m)$ decays exponentially for large m. At $\rho = \rho_c(w)$, $P(m)$ decays as a power law $P(m) \sim m^{-\tau}$ for large m, where the exponent τ is the same everywhere on the critical line $\rho_c(w)$. A more striking and interesting behaviour occurs for $\rho > \rho_c(w)$. In this phase, $P(m)$ decays as the same power law $\sim m^{-\tau}$ for large m as at the critical point, but in addition develops a delta function peak at $m = \infty$. Physically this means that an infinite aggregate forms that subsumes a finite fraction of the total mass, and coexists with smaller finite clusters whose mass distribution has a power law tail. In the language of sol-gel transitions, the infinite aggregate is like the gel while the smaller clusters form the sol. However, as opposed to models of irreversible gelation where the sol disappears in the steady state, in our model the gel coexists with the sol, which has a power law distribution of mass. Interestingly, the

mechanism of the formation of the infinite aggregate in the steady state resembles Bose–Einstein condensation (BEC), though the condensate (the infinite aggregate here) forms in real space rather than momentum space as in conventional BEC.

This nontrivial dynamical phase transition occurs in both SCA and ACA in all spatial dimensions d including $d=1$. We expect that the exponent τ depends on the dimension d but is universal with respect to lattice structures and initial conditions. However, the bias in the movement of masses that distinguishes the two models SCA and ACA is a relevant perturbation and the corresponding exponents τ_s (for SCA) and τ_{as} (for ACA) differ from each other.

We comment on the relationship of our model and results to earlier work on related models.

(i) Takayasu and coworkers have studied[8] a lattice model where masses diffuse and aggregate upon contact as in our model. However our model differs from the Takayasu model in the following important way. In that model there is a nonzero rate of injection of a single unit of mass from the outside into each lattice site, whereas in our model the injection move is replaced by the "chipping" of a single unit of mass to a neighbouring lattice site. Thus in our model total mass is conserved as opposed to the Takayasu model where total mass increases linearly with time. In the Takayasu model the mass distribution $P(m)$ has a power law decay in the steady state[8] but there is no phase transition as in our conserved model. Finally, while the directed and undirected versions of the Takayasu model evolve in the same way, in our model directionality in motion changes the universality class.

(ii) In the context of gelation, Vigil, Ziff and Lu[9] studied models of coagulation and single-particle break off within a rate equation approach. There is, however, a significant point of difference from our model: in our model, the coagulation kernel is independent of mass, while in ref. 9 it is proportional to the product of the two coagulating masses. The latter feature strongly enhances the tendency towards aggregation, and leads to the formation of an infinite aggregate (gel) in a finite time while in our model an infinite aggregate forms only in the steady state.

(iii) Krapivsky and Redner (KR)[10] studied a model of coagulation (with a mass independent kernel) and single-particle break off, within a rate equation approach. Our model is different, in that in addition to aggregation and single-particle break off, it allows for diffusion of masses, and is defined on a lattice. Besides, even within mean field theory (neglecting diffusion), our model differs from KR in detailed moves. Despite this, the leading asymptotic behaviours of our mean field equations (Section III)

are similar to those of KR, reflecting the fact that the mean field equations in both cases conserve mass. KR found that the asymptotic mass distribution decays exponentially in one phase, while it decays as a power-law in the other phase. However the occurrence of a Bose–Einstein condensation like effect, leading to an infinite aggregate in the power law phase, was not pointed out explicitly in ref. 10, though it was implicit in their equations.

An important point of difference between KR and the present work is that we allow for diffusion of particles. This quantitatively changes the critical exponent characterizing the asymptotic behaviour of the mass distribution in lower dimensions, in particular for $d = 1$, which we study in detail (Section IV).

(iv) Models of vacancy cluster formation consider the attachment and detachment of single vacancies to clusters,[11] often with rates that depend on the cluster size. This would correspond to allowing only chipping moves in our model (Section V A). Since cluster aggregation moves are absent in this case, there is no tendency to form very large clusters and the mass distribution decays exponentially with m.

(v) Recently, lattice gas models have been proposed[12] to describe the distribution of droplets in fast-expanding systems such as in the fragmentation process following a nuclear collision. The distribution of fragments shows a pronounced peak at the large mass end, reminiscent of our infinite aggregate. However, the distribution of the remaining fragments decays exponentially, and not as a power law as in our case.

(vi) Bose–Einstein-like condensation in real space has also been found in lattice gas models of traffic[13, 14] in which different cars have different maximum speeds, chosen from an *a priori* specified distribution. This corresponds to phase separation into high density and low density regions, a phenomenon which is also found when randomness in hopping rates is associated with points in space, rather than with cars.[15, 16] An important difference between these studies and ours is that they involve quenched disorder (the assignment of different maximum speeds, either to cars, or to different lattice sites), whereas the BEC phenomenon in our case occurs in the absence of disorder, in a translationally invariant system.

It should be pointed out that BEC is also found in other translationally invariant systems, which however differ from the present model in important respects. For instance, the balls-in-boxes backgammon model[17] which shows BEC is an equilibrium model with infinite ranged moves, in contrast to the nonequilibrium short-ranged model under consideration here. Finally, the bus-route model[18] exhibits BEC, but a strict transition is obtained in that model only in the limit in which a certain local rate

$\lambda \to 0$, whereas our model exhibits BEC over a wide range of parameter space.

III. MEAN FIELD THEORY

In this section, we study the conserved mass models within the mean field approximation which keeps track only of the distributions of masses, ignoring correlations in the occupancy of adjacent sites. The mean field theory is identical for both the symmetric and asymmetric models. This is a defect of the MF approximation as, in fact, the existence of a nonzero mass current in the asymmetric model affects fluctuations in an important way. Although MF theory misses this important aspect of the physics, it is still instructive since it reproduces the phase diagram correctly, at least qualitatively. Besides, in high dimensions where fluctuations are negligible, the MF theory captures the correct physics even quantitatively.

Ignoring correlations between masses at neighbouring sites on the lattice, one can directly write down the evolution equation for $P(m, t)$, the probability that any site has a mass m at time t,

$$\frac{dP(m,t)}{dt} = -(1+w)[1+s(t)]\,P(m,t) + wP(m+1,t) + ws(t)\,P(m-1,t) + P * P; \qquad m \geqslant 1 \tag{1}$$

$$\frac{dP(0,t)}{dt} = -(1+w)\,s(t)\,P(0,t) + wP(1,t) + s(t) \tag{2}$$

Here $s(t) \equiv 1 - P(0, t)$ is the probability, that a site is occupied by a mass and $P * P = \sum_{m'=1}^{m} P(m', t)\,P(m-m', t)$ is a convolution term that describes the coalescence of two masses.

The above equations enumerate all possible ways in which the mass at a site might change. The first term in Eq. (1) is the "loss" term that accounts for the probability that a mass m might move as a whole or chip off to either of the neighbouring sites, or that a mass from a neighbouring site might move or chip off to the site in consideration. The probability of occupation of the neighbouring site, $s(t) = \sum_{m=1}^{M} P(m, t)$, multiplies $P(m, t)$ within the mean-field approximation where one neglects the spatial correlations in the occupation probabilities of neighbouring sites. The remaining three terms in Eq. (1) are the "gain" terms enumerating the number of ways that a site with mass $m' \neq m$ can gain the deficit mass $m - m'$. The second equation Eq. (2) is a similar enumeration of the possibilities for loss and gain of empty sites. Note that the coordination number of the lattice does not appear explicitly in the above equations as the rates of hopping

(of either a single unit or the mass as a whole) to neighbours are defined with respect to movements from or onto sites, and not across bonds.

Evidently, the MF equations conserve the total mass. Thus there are two parameters in the model, namely the conserved mass density $\rho = \sum mP(m)$ and the chipping rate w.

Equations (1) and (2) incorporate the same physical processes as KR,[10] though their rate equations differ from (1) and (2) in details. For instance in KR, single particles which break off from a mass do not immediately recombine with other masses, but form a reservoir of $m = 1$ particles; these unit masses subsequently coagulate with other masses. In our case, by contrast, single particles which chip off to an already occupied site immediately recombine with the mass on that site. Despite these differences, we will see below that the behaviour of $P(m)$ for large m is similar. We also note that the chipping rate w was set to unity in KR. In our model, we can explore the phase diagram in the full $\rho - w$ plane which has the advantage that we can study limiting points such as $w \to 0$ or $w \to \infty$ corresponding to exactly solvable models even when diffusion is included (see Section V).

We solve the equations (1) and (2) by a generating function technique. Since this calculation has appeared earlier,[7] here we discuss only the results.

We find that for fixed w, there is a phase transition at a critical density $\rho_c = \sqrt{w+1} - 1$.

(i) For $\rho < \rho_c$, the asymptotic mass distribution falls as

$$P(m) \sim e^{-m/m^*}/m^{3/2} \tag{3}$$

where the characteristic mass m^* diverges as $\rho \to \rho_c$.

(ii) For $\rho = \rho_c$,

$$P(m) \sim m^{-5/2} \tag{4}$$

for large m.

(iii) For $\rho > \rho_c$, the fractional number of occupied sites does not increase but remains stuck at the value $s_c = (w + 2 - 2\sqrt{w+1})/w$. The excess density is accommodated in an infinite-mass aggregate so we may write

$$\rho = \frac{w}{2}(1 - s_c) + \rho_\infty \tag{5}$$

where ρ_∞ is the fraction of the mass in the infinite aggregate. The mechanism of the formation of the aggregate is reminiscent of Bose–Einstein condensation. In that case, for temperatures in which a macroscopic condensate exists, particles added to the system do not contribute to the occupation of the excited states; they only add to the condensate, as they do to the infinite aggregate here.

IV. NUMERICAL SIMULATION IN ONE DIMENSION

In order to see if the MF phase diagram remains at least qualitatively correct in lower dimensions, we have studied both SCA and ACA using Monte Carlo simulations on a one-dimensional lattice with periodic boundary conditions. Although we present results here for a relatively small size lattice, $N = 1024$, we have checked our results for larger sizes as well. We confirmed that all the qualitative predictions of the mean-field theory remain true in 1-d though the exponents change from their MF values.

Figure 1 displays two numerically obtained plots of $P(m)$ in the steady state of SCA. For fixed $w = 1.0$, we have measured $P(m)$ for two values of the density, namely $\rho = 0.2$ and $\rho = 3.0$. For $\rho = 0.2$, we find exponential decay of $P(m)$ (denoted by $\times$ in Fig. 1). For $\rho = 3.0$, $P(m)$ decays as a power law (denoted by $+$ in Fig. 1) which is cut off by finite size effects but in addition, there is a sharp peak at a much larger mass signalling the existence of the "infinite" aggregate as predicted in the MF theory. We confirmed that the mass M_{agg} in this aggregate grows linearly with the size, and that the spread δM_{agg} grows sublinearly, implying that the ratio $\delta M_{agg}/M_{agg}$ approaches zero in the thermodynamic limit. Further, the cutoff on the power-law part of the distribution also grows sublinearly with size, so its separation from the aggregate peak also grows with increasing size (see Fig. 1). As one decreases ρ for fixed w, the mass M_{agg} decreases and finally vanishes at the critical point, $\rho_c(w)$ where $P(m)$ only has a power law tail. For $w = 1$, we find numerically $\rho_c(1) \approx 0.39$. In the inset of Fig. 1, we plot the numerical phase boundary in the (ρ, w) plane (denoted by closed circles). For comparison, we also plot the MF phase boundary $\rho_c(w) = \sqrt{(w+1)} - 1$. In fact, it can be shown that the mean-field $\rho_c(w)$ is exact for the $d = 1$ SCA.[19]

In Fig. 2 and in its inset, we present similar plots for the asymmetric model ACA. Here the steady state mass distribution function $P(m)$ is plotted for two values of the density $\rho = 0.2$ and $\rho = 10.0$ with fixed $w = 1.0$. In the first case, $P(m)$ decays exponentially whereas in the second case it has a power law tail and in addition the "infinite" aggregate as in the case of SCA.

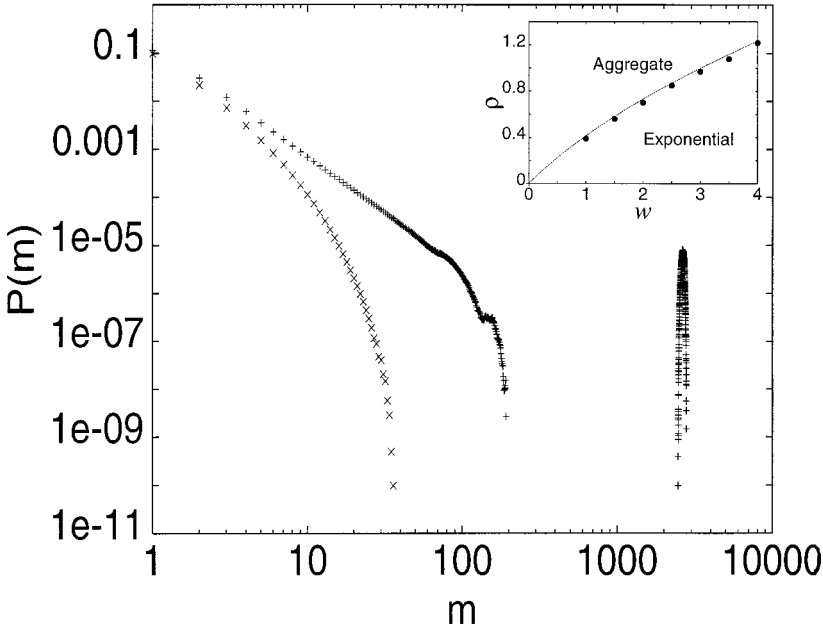

Fig. 1. log–log plot of $P(m)$ vs. m for SCA for two choices of the parameters: $(w = 1.0, \rho = 0.2)$ and $(w = 1.0, \rho = 3.0)$ on a periodic lattice of size $N = 1024$. Inset: Phase diagram. The solid line and the points indicate the phase boundary within mean field theory and 1-d simulation respectively.

The exponent τ_s for SCA which characterizes the finite-mass fragment power law decay for $\rho > \rho_c(w)$ is numerically found to be 2.33 ± 0.02 and remains the same at the critical point $\rho = \rho_c(w)$. In the asymmetric model ACA, we find the corresponding exponent $\tau_{as} \approx 2.05$ within numerical error. Note however that because the total mass and hence the mass density, $\rho = \sum mP(m)$ is conserved and finite, the decay of $P(m)$ must be faster than m^{-2} for large m to avoid ultraviolet divergence. In ACA the numerical value of τ_{as} in 1-d is very close to 2 suggesting perhaps that $P(m)$ decays as m^{-2} with additional logarithmic corrections such that ρ remains finite. But within our simulations, it is not easy to detect these additional logarithmic factors. Thus clearly in 1-d, SCA and ACA belong to different universality classes.

V. MAPPING TO A LATTICE GAS MODEL IN ONE DIMENSION

In this section, we show that in one dimension the mass model studied above can be mapped exactly onto a lattice gas (LG) model consisting of

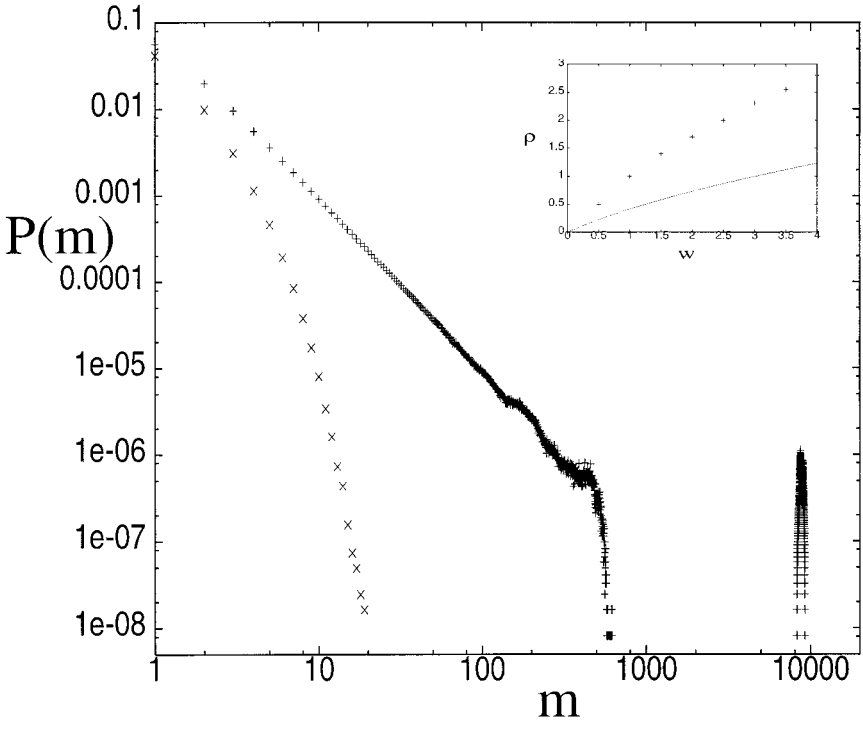

Fig. 2. log–log plot of $P(m)$ vs. m for ACA for two choices of the parameters: $(w = 1.0, \rho = 0.2)$ and $(w = 1.0, \rho = 10.0)$ on a periodic lattice of size $N = 1024$. Inset: Phase diagram. The solid line and the points indicate the phase boundary within mean field theory and 1-d simulation respectively.

particles and holes. In the language of the LG model, it is somewhat easier to understand the two phases and the transition between them. Besides, for certain limiting values of the parameters, the steady state of the LG model can be solved exactly.

Consider the mass model (both SCA and ACA) on a ring R of N lattice sites. Let m_i denote the mass at site i of R in a given configuration. Let $M = \sum_{i=1}^{N} m_i$ denote the total mass on R. We first construct a new ring R' consisting of $L = N + M$ sites. For every lattice site i of ring R, we put a particle (labeled by i) on ring R' such that the ith and $(i+1)$th particle on R' are separated exactly by m_i holes. The ring R' will therefore have N particles and M holes. Also by construction, these particles on R' are hard core, i.e., any site of R' can contain at the most one particle. Thus every mass configuration on R maps onto a unique particle-hole configuration on R'. In Fig. 3, we give an example of this mapping. We also note that

particle density ρ' on R' is simply related to the mass density ρ on R via, $\rho' = N/(N+M) = 1/(1+\rho)$.

Given this exact mapping between configurations, we now examine the correspondence between the mass dynamics on R and the particle dynamics on R'. Consider a pair of neighbouring sites $(i-1)$ and i on R where the masses are m_{i-1} and m_i. This translates to having m_{i-1} holes to the right of $(i-1)$th particle and m_i holes to the right of ith particle on R'. Consider first the chipping move that occurs with rate p_2 (Fig. 3). If a single unit of mass chips off the $(i-1)$th site and moves to ith site (i.e., $m_{i-1} \to m_{i-1} - 1$ and $m_i \to m_i + 1$) on R, it corresponds to the ith particle on R' hopping to its neighbouring site to the left with rate p_2. Similarly, the reverse move (i.e., $m_i \to m_i - 1$ and $m_{i-1} \to m_{i-1} + 1$) corresponds to the ith particle on R' hopping one step to the right with rate p_2. Thus the

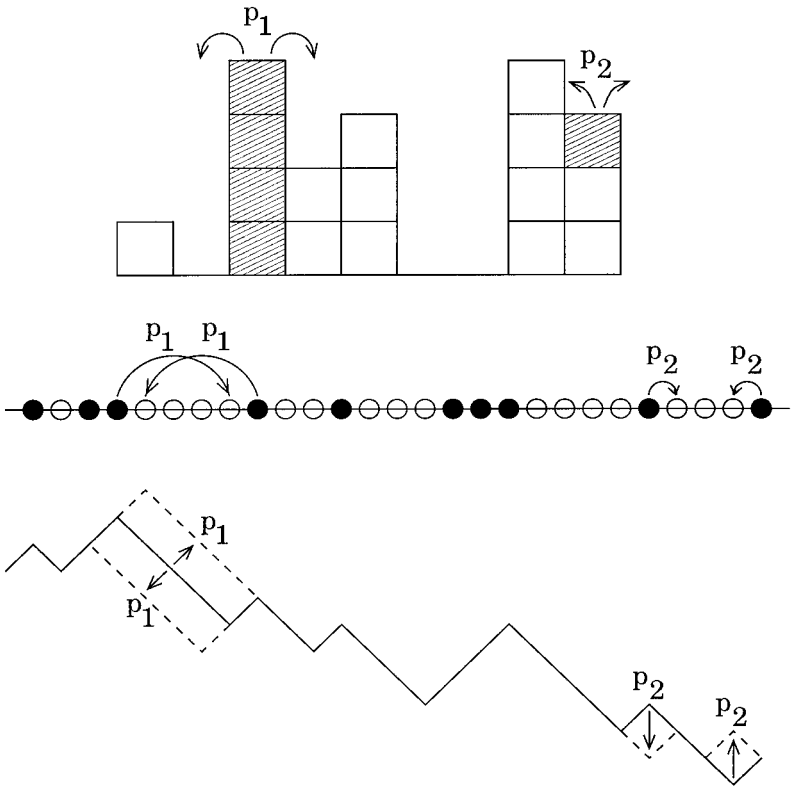

Fig. 3. The constructions of the equivalent lattice gas model and interface model are illustrated for a particular configuration of the conserved mass model. The shaded blocks indicate the masses that would move as a result of "diffusion and aggregation" and "chipping."

chipping move of SCA on R corresponds precisely to the "symmetric exclusion process" (SEP)[20] on R' where a particle can hop to its nearest neighbour on either side provided the neighbour is empty. Similarly the chipping move of ACA on R corresponds exactly to the "asymmetric exclusion, process" (ASEP)[20, 21, 25] on R' where particles move only along one direction on R'.

But in addition to chipping, we also have the diffusion and aggregation move in the mass model that occurs with rate p_1 (as shown for the block of particles in Fig. 3). For a pair of sites $(i-1)$ and i with respective masses m_{i-1} and m_i on R, suppose the whole mass m_{i-1} moves to the ith site (i.e., $m_{i-1} \to 0$ and $m_i \to m_i + m_{i-1}$). This would mean that on R', the ith particle jumps to the farthest available hole (without crossing the $(i-1)$th particle) to its left with rate p_1. Similarly the reverse move, $m_i \to 0$ and $m_{i-1} \to m_{i-1} + m_i$, would translate on R' to the ith particle jumping to the farthest available hole to its right (without crossing the $(i+1)$th particle) with rate p_1. In the asymmetric version of the model, the particle can jump to the farthest available hole (without crossing the next particle) in one direction only.

To summarize, in our LG model we have hard core particles with particle density ρ'. The world lines of particles cannot touch or cross each other due to their hard core nature. There are two possible moves for each particle. With rate p_2, a particle moves to its adjacent site (if it is empty) and with rate p_1 the particle jumps to the farthest available hole maintaining the hard core constraint. In SCA, the particle can hop with equal probability to the left or right while in ACA, it hops only in one direction, say to the right. In this LG language, it is the competition between the short range and long range hopping of the particles that is responsible for the phase transition. As in the mass model, the only two parameters of the model are the ratio of the two rates $w = p_2/p_1$ and the density of particles ρ'. We also note that $P(m)$ in the mass model corresponds to the size distribution of hole clusters in the LG model.

In the following we fix the density of particles ρ' and study the two extreme limits $w \to \infty$ and $w = 0$ where exact results can be obtained.

A. Only Chipping: $w \to \infty$

Since $w = p_2/p_1$, the limit $w \to \infty$ corresponds to $p_1 = 0$ with p_2 remaining nonzero. This means only chipping moves are allowed in the mass model. As mentioned in Section II, in this limit the model has some resemblance to models of vacancy cluster formation,[11] with mass in our model representing the number of vacancies in a cluster. Chipping off from

clusters with $m \geqslant 2$ corresponds to vacancy detachment, whereas the chipping move for $m = 1$ is tantamount to either diffusive hopping (if the neighbouring site is empty), or to attachment to a cluster (if the neighbouring site has a mass on it).

In the LG version, the "only-chipping" model corresponds to just the exclusion process[20, 21] either symmetric (SEP) (corresponding to SCA) or asymmetric (ASEP) (corresponding to ACA). For both SEP and ASEP all configurations are equally likely in steady state, implying product measure in the thermodynamic limit.[20, 21] The probability $P(m)$ of having exactly m holes following a particle is simply given by $P(m) = \rho'(1-\rho')^m$. Using $\rho' = 1/(1+\rho)$, we thus obtain an exact result for $P(m)$ of the mass model in the $w \to \infty$ limit,

$$P(m) = \frac{\rho^m}{(1+\rho)^{m+1}} \tag{6}$$

which clearly demonstrates the exponential decay of $P(m)$ for large m.

We note in passing that Eq. (6) also describes the distribution of masses in any dimension in an "only chipping" model in which the rate of chipping at site i is proportional to the mass m_i on that site. In this case, evidently every unit of mass performs a simple random walk, and the problem is tantamount to that of M independent random walkers on the lattice. Standard methods of statistical mechanics can then be used to describe the steady state. The grand partition function is then

$$Z = (1 + z + z^2 \cdots)^N = \frac{1}{(1-z)^N} \tag{7}$$

where z is the fugacity, and the probability of finding m particles on a site is

$$P(m) = (1-z)\, z^m \tag{8}$$

Eliminating z in favour of $\rho = z/(1-z)$, we see that Eq. (8) reduces to Eq. (6).

B. No Chipping: $w = 0$

We now consider the other limit $w = 0$ where there is no chipping and the masses only diffuse as a whole and aggregate with each other. In the LG language, this would mean that particles undergo only long range hopping to the farthest available hole (without crossing the next particle).

In order to find the exact steady state in this limit, we first consider the mass model on a finite ring R of N sites and total mass $M = \rho N$. As time progresses, masses diffuse and coagulate with each other and the number of empty sites increases. Since the diffusive motion confined in a finite region of space is ergodic, eventually all the masses will coagulate with each other and there will be precisely one single big conglomerate with mass M which will move on the ring. Thus in the steady state, one gets exactly, $P(m) = \delta(m - \rho N)$. In the LG language, this would mean that on a finite lattice, the particles and holes will become completely phase separated in the steady state.

It is also useful to study the approach to this phase separated steady state. We first note that on an infinite 1-d lattice, the time dependent single site mass distribution function, $P(m, t)$ can be exactly solved in the $w = 0$ limit.[27] It was shown exactly in ref. 27 that in the scaling limit, $m \to \infty$, $t \to \infty$ but keeping $m/\sqrt{t}$ fixed, the function $P(m, t) \sim t^{-1/2} S(m/c\sqrt{t})$ where the constant c depends on the initial condition but the scaling function $S(x)$ is universal and is given by

$$S(x) = \frac{\pi x}{2} \exp\left[-\frac{\pi x^2}{4} \right] \tag{9}$$

In the LG model, this would mean that as time progresses, the system undergoes phase separation and breaks into domains of particles and holes. The average linear size of these domains grows with time as $l(t) \sim t^{1/2}$ at late times. At this point it is useful also to note that in usual models of coarsening with locally conserved dynamics, the domain size grows as $l(t) \sim t^{1/3}$ [28] as opposed to $t^{1/2}$ here. This, however, is not entirely surprising since in our model, even though the particle number is conserved globally, the long range hopping effectively reduces this to a locally non-conserved model with growth law $t^{1/2}$. Similar behaviour was noticed earlier in other models of coarsening with globally conserved dynamics.[29] In an infinite system the domain size keeps growing indefinitely as $l(t) \sim t^{1/2}$. However in a finite lattice of L sites, when $l(t) \sim L$ after a time $t \sim L^2$, the domains stop growing and the system eventually breaks up into two domains only, one of particles and the other of holes. We note that all the conclusions reached in this subsection are equally valid for both symmetric and asymmetric versions of the model.

To summarize this section, we find that for fixed ρ in one dimension, the two extreme limits $w \to 0$ and $w \to \infty$ are exactly solvable for their steady states. In the limit $w \to 0$, the system has a phase separated steady state in the LG model which in the mass model corresponds to having a single massive aggregate. In the other limit $w \to \infty$, the LG corresponds

to the simple exclusion process with product measure steady state, which corresponds to an exponential mass distribution in the mass model. Thus there is a competition between the long range hopping that tends to create phase separation and the short range hopping that tends to mix the particles and holes to produce a product measure steady state. As w is increased from 0 for fixed ρ, the massive aggregate coexists with power law distributed smaller masses (or hole clusters in the LG language) up to some critical value $w_c(\rho)$. For $w > w_c(\rho)$, the massive aggregate disappears and the cluster size distribution of holes becomes exponential.

VI. DYNAMICS IN ONE DIMENSION: MAPPING TO INTERFACE MODELS IN (1+1) DIMENSION

In the previous sections we have studied the static properties of the model in the steady state. However it is also important to study the dynamics of the model in the steady state. The universal features of the dynamics is usually best captured by time dependent correlation functions in the steady state. In this section we however take a slightly different route. Instead of studying the time-dependent correlation functions directly in the mass or the equivalent lattice gas model, we first map the LG model onto an interface model and then study the time dependent properties of the width of the fluctuating interfaces. The advantage of this route is that not only does it capture the essential universal features of the dynamics, but it also makes contact with other well studied interface models in certain limiting cases.

There is a standard way[21] to map a LG configuration in one dimension to that of an interface configuration on a 1-d substrate. One defines a new set of variables $\{S_i\}$ such that $S_i = 1$ if the ith site is occupied by a particle and $S_i = -1$ if it is empty. Then the interface height h_i at site i is defined as, $h_i = \sum_{j=1}^{i} S_j$. Thus the overall tilt of the interface, $\tan\theta = (h_L - h_1)/L = 2\rho' - 1$ is set by the particle density ρ' in the LG model.

The different dynamical moves in the LG model can be translated in a one to one fashion to corresponding moves of the interface. For example, if a particle at site i jumps one unit to the right, it corresponds to the decrease of height h_i by 2 units, $h_i \to h_i - 2$. Similarly, if the particle at site $(i+1)$ jumps one unit to the left, the height h_i increases by 2 units, $h_i \to h_i + 2$. Thus the nearest neighbour hopping of particles to the left or right in the LG model corresponds respectively to deposition and evaporation moves in the interface model. Similarly the long range hopping of a particle to the farthest available hole before the next particle would translate to nonlocal moves in the interface as shown in Fig. 3. Once again, the

ratio of the rates of evaporation-deposition moves to that of the nonlocal moves is given by the parameter w.

A natural measure of the fluctuations of the interface is its width defined for a finite system of size L as,

$$W(L, t) = \sqrt{\frac{1}{L} \sum_{i=1}^{L} [h_i - \bar{h}]^2} \tag{10}$$

where $\bar{h} = \sum_{i=1}^{L} h_i/L$. The width $W(L, t)$ is expected to have a scaling form,[21]

$$W(L, t) \sim L^{\chi} F(t/L^z) \tag{11}$$

in the scaling limit with large L, large t but keeping t/L^z finite. The exponents χ and z are respectively the roughness and the dynamical exponents and the scaling function $F(x)$ is universal with the asymptotic behaviour: $F(x) \to O(1)$ as $x \to \infty$ and $F(x) \sim x^{\beta}$ as $x \to 0$ where $\beta = \chi z$. The exponents χ and z characterize the universality classes of the interface models.

In the following we keep the particle density ρ' fixed and investigate the width of the corresponding interface model $W(L, t)$ by varying the parameter w. How do the exponents χ and z that characterize the universal behaviour of interface fluctuations change as one varies w from 0 to ∞? We study this question for both the symmetric and the asymmetric models and denote the respective exponents by $(\chi_w^{(s)}, z_w^{(s)})$ and $(\chi_w^{(as)}, z_w^{(as)})$. In the following three subsections, we study the width $W(L, t)$ in both models for three special values of w, namely $w \to \infty$, $w = 0$ and $w = w_c(\rho')$. In the first two cases we find analytical results whereas in the last case, we present numerical results only.

A. Only Chipping: $w \to \infty$

We first consider the symmetric mass model SCA whose lattice gas equivalent corresponds to the SEP in the $w \to \infty$ limit as noted in Section V. This means that in the corresponding interface model, nonlocal moves are absent and the only allowed moves are evaporation and deposition subject to certain local constraints. An important property of this symmetric model is that the average velocity of the interface is zero as the evaporation and deposition occurs with equal probability. It is well known[21] that the continuum version of this discrete interface model corresponding to SEP is well described by the Edwards–Wilkinson equation.[22, 23]

This linear evolution equation can be easily solved and one gets the exact exponents,[22, 23]

$$\chi_{\infty}^{(s)} = \tfrac{1}{2}; \qquad z_{\infty}^{(s)} = 2 \tag{12}$$

The LG equivalent of the asymmetric mass model ACA in the $w \to \infty$ limit is the ASEP. In the corresponding interface model the allowed moves are either only deposition or only evaporation (but not both) depending upon the direction of particle motion in ASEP. Thus the interface has a nonzero average velocity and its continuum version is known[21] to be described by the nonlinear KPZ equation.[24] In one dimension, the KPZ equation can be solved exactly and the exponents are known to be,[24]

$$\chi_{\infty}^{(as)} = \tfrac{1}{2}; \qquad z_{\infty}^{(as)}(as) = \tfrac{3}{2} \tag{13}$$

Thus in the limit $w \to \infty$, our model reduces to two known interface models for symmetric and asymmetric cases respectively and the corresponding exponents are obtained exactly.

B. No Chipping: $w = 0$

We have mentioned in Section V that in the $w \to 0$ limit, as time progresses the LG phase separates into domains of particles and holes. In the equivalent spin representation where a particle is represented by an up spin, $S_i = 1$ and a hole by a down spin, $S_i = -1$, this then represents a spin model coarsening with time with average domain size growing as $l(t) \sim t^{1/2}$. In a finite system of length L, eventually the system breaks up into two domains of opposite signs. In the interface representation, this would mean that the system would develop a single mound. Mound formation has also been studied recently in other interface models.[26]

We note from Eq. (10) and the definition, $h_i = \sum_{j=1}^{i} S_j$ that the calculation of the width $W(L, t)$ requires the expression for the equal time spin correlation function, $\langle S(i, t)\, S(j, t) \rangle$ in the equivalent spin model. From the general theory of coarsening it is known[28] that for $l(t) \ll L$, the equal time spin correlation function satisfies the scaling behaviour, $\langle S(0, t)\, S(r, t) \rangle \sim G(r/l(t))$. We have assumed that the system size L is large so that translational invariance holds in the bulk of the system. Using this scaling form in Eq. (10) and the result $l(t) \sim t^{1/2}$, a simple power counting gives $W(L, t) \sim LF(t/L^2)$. Thus for $w = 0$, we have the exponents,

$$\chi_0 = 1; \qquad z_0 = 2 \tag{14}$$

for both the symmetric and asymmetric models. The roughness exponent $\chi_0 = 1$ can be easily understood from the fact that in the steady state the system develops a single mound whose maximum height is of $O(L)$ and hence the width of the fluctuations is also of order L.

C. Critical Point: $w = w_c(\rho)$

In this subsection, we keep the density $\rho' = 1/(1+\rho)$ fixed and tune w to its critical value, $w = w_c(\rho)$ and calculate the width $W(L, t)$ of the interface. Unfortunately we are unable to obtain any analytical result for this critical case and will only present numerical estimates.

We first consider the symmetric model. In this case we fix $\rho = 1$. In the LG language this means particle density, $\rho' = 1/2$. We first estimate the

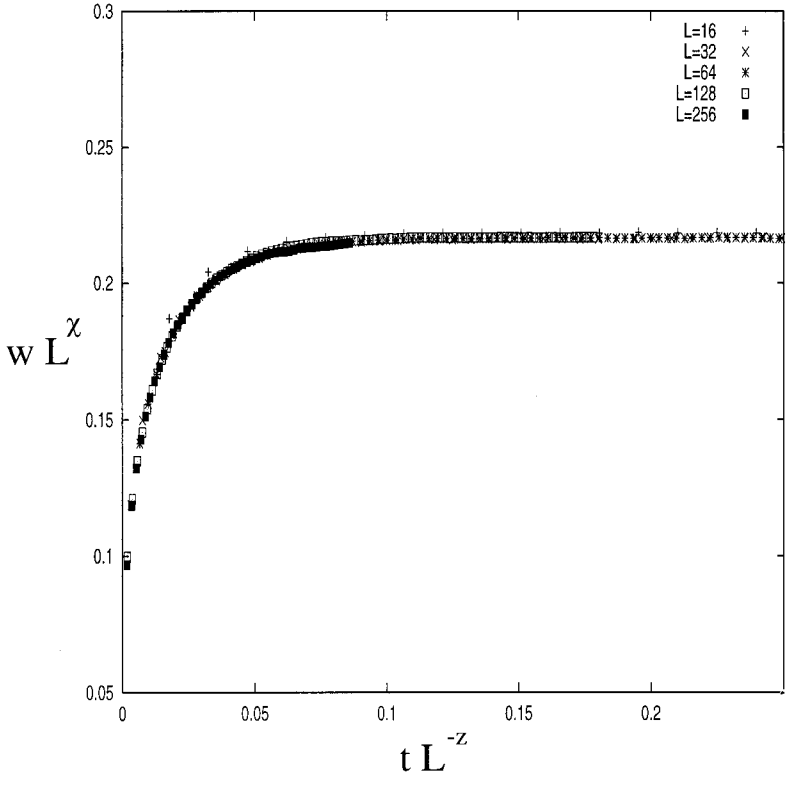

Fig. 4. The scaled width W/L^{χ} is plotted against the scaled time t/L^{z} for lattice sizes $L = 16$, 32, 64, 128 and 256 at the critical point $\rho = 1$, $w_c \approx 3.35$) of the interface corresponding to SCA. The best data collapse is obtained with the choice of exponent values, $\chi \approx 0.67$ and $z \approx 2.1$.

critical point, $w_c(\rho = 1) \approx 3.35$ by simulating the equivalent mass model. Next we fix the value of $\rho = 1$ and $w = 3.35$ in the interface model and measure the width $W(L, t)$ for different lattice sizes, $L = 16$, 32, 64, 128 and 256. In order to verify the scaling form, $W(L, t) \sim L^{\chi_c} F(t/L^{z_c})$, we plot in Fig. 4, W/L^{χ_c} as a function of t/L^{z_c} for different L. The best collapse of data is obtained with the choice, $\chi_c^{(s)} \approx 0.67$ and $z_c^{(s)} \approx 2.1$. The asymmetric case however is much more complicated due to the possible existence of logarithmic factors in one dimension and perhaps also due to other strong corrections to scaling. Proceeding as in the symmetric case, we first estimate the critical point, $w_c(\rho = 1) \approx 0.77$ and measure the width $W(L, t)$. In this case we did not find a good data collapse using the canonical scaling form, $W(L, t) \sim L^{\chi} F(t/L^{z})$. Instead we tried collapsing the data assuming, $W(L, t) \sim W_{st} F(t/L^{z})$ where W_{st} is the steady state width $W(L, \infty)$. This gives a somewhat better convergence to the collapse as L increases as shown in Fig. 5 with the choice $z \approx 1.67$. In the inset, we plot W_{st} vs. L. It is difficult to estimate the asymptotic growth $W_{st} \sim L^{\chi}$

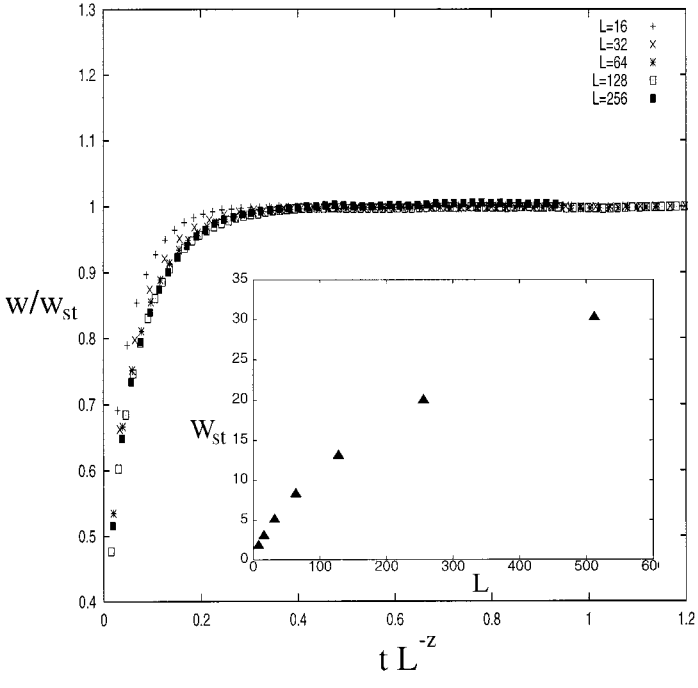

Fig. 5. The scaled width W/W_{st} is plotted against the scaled time t/L^{z} for lattice sizes $L = 16$, 32, 64, 128 and 256 at the critical point ($\rho = 1, w_c \approx 0.7$) of the interface corresponding to ACA. The best convergence to data collapse as L increases is obtained with the choice $z \approx 1.67$. Inset shows W_{st} plotted against L.

(possibly with a logarithmic corrections) from the available data. A naive linear fit to the log–log plot of W_{st} vs. L gives an estimate of the slope, $\chi \approx 0.68$. Thus given the available data, we find the approximate estimates for the exponents, $\chi_c^{(as)} \approx 0.68$ and $z_c^{(as)} \approx 1.67$ at the critical point of the asymmetric model. However these are just approximate estimates and one needs larger scale simulations to determine the exponents more accurately for the asymmetric model.

D. Flows

We have also studied the width $W(L, t)$ numerically for other values of w. This includes the numerical verification of analytical predictions for the exponents in the limit of small and large w. We do not present here all these details but summarize the main picture that emerges from these studies by means of the schematic flow diagram shown in Fig. 6.

We find three different sets of exponents (χ, z) that characterize the behaviour in three regions on the w axis for fixed ρ: subcritical when $w < w_c(\rho)$, critical when $w = w_c(\rho)$ and supercritical when $w > w_c(\rho)$. The subcritical regime is controlled by the aggregation fixed point (denoted AGG in Fig. 6) at $w = 0$, i.e., the phase separation fixed point with $\chi = 1$ and $z = 2$ for both symmetric and asymmetric models. The supercritical regime is controlled by the fixed point at $w \to \infty$. For the symmetric case, this is the Hammersley–Edwards–Wilkinson fixed point HEW ($\chi = 1/2$, $z = 2$), whereas in the asymmetric case this is the KPZ fixed point ($\chi = 1/2$, $z = 3/2$). The fixed points SC and ASC in Fig. 6 correspond to criticality in the symmetric and asymmetric conserved mass models respectively; these

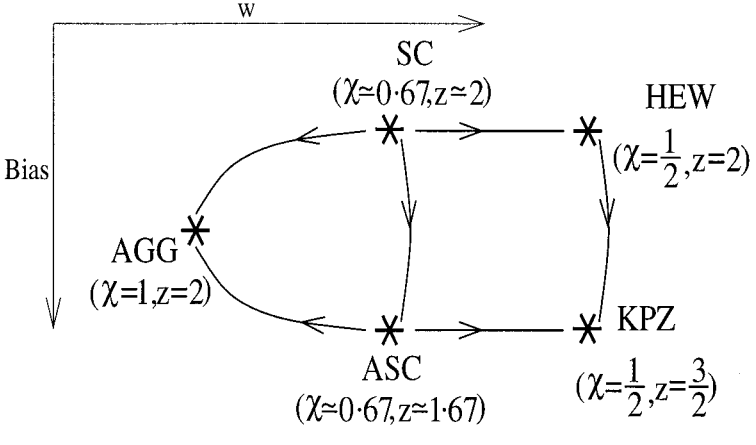

Fig. 6. Schematic depiction of fixed points and associated flows.

are new unstable fixed points with exponents, ($\chi \approx 0.67, z \approx 2.1$) for the symmetric case and ($\chi \approx 0.68, z \approx 1.67$) for the asymmetric case respectively.

VII. GENERALIZATION TO ARBITRARY FRAGMENTATION KERNEL: RELATION TO OTHER MODELS

In the mass model discussed so far we have considered only two possible moves, namely "chipping" of a single unit of mass to a neighbouring site with rate w or hopping of the mass as a whole to a neighbouring site with rate 1. However in a more general setting, k units of mass can break off a mass m and hop to a neighbouring site with rate $p(k \mid m)$ where $k \leqslant m$. In the equivalent lattice gas version in one dimension, this would mean the hopping of a particle with rate $p(k|m)$ to the kth hole to the right or left without crossing the next particle which is located at a distance $m+1$. In the asymmetric version, the particles jump only along one direction as usual (either left or right). In the model studied so far,

$$p(k \mid m) = w\delta_{k,1} + \delta_{k,m} \tag{15}$$

where δ_{ij} is the Kronecker delta function. With this mass fragmentation kernel, we have seen that in the steady state the system undergoes a non-equilibrium phase transition as the parameter w that controls the relative strength of the two delta peaks is varied.

The question naturally arises as to whether this phase transition exists for other fragmentation kernels $p(k \mid m)$. In general, it is hard to find the steady state analytically for arbitrary $p(k \mid m)$. However, for some special choices of the kernels, it is possible to obtain exact steady states via mappings to some other solvable models of statistical mechanics. Below we list a few of them.

In the context of traffic models, Klauck and Schadschneider recently studied[30] an asymmetric exclusion process in one dimension where a particle can jump either to the neighbouring hole to the right with rate p_1 or to the second hole to the right with rate p_2. The corresponding jump kernel can be written as

$$p(k \mid m) = p_1\delta_{k,1} + p_2\delta_{k,2} \tag{16}$$

By generalizing the matrix product ansatz used for ASEP,[33] the steady state of this model was shown[30] to have simple product measure for all p_1 and p_2. Using this result, it is easy to show that in the corresponding mass model with mass density ρ, the steady state single site mass distribution $P(m)$ (the same as the probability of having a hole cluster of size m in the

LG model) is simply given by, $P(m) = \rho/(1+\rho)^{m+1}$ and therefore decays exponentially for large m for arbitrary p_1 and p_2.

Recently Rajesh and Dhar studied[31] an anisotropic directed percolation model in 3 dimensions. Their model can be reduced to an asymmetric hard core LG model with the following jump kernel,

$$p(k \mid m) = p^{1-\delta_{k,0}}(1-p)^{m-k} \tag{17}$$

where $0 \leqslant p \leqslant 1$. By mapping it to the five vertex model, the steady state of this model was shown exactly to have a simple product measure for all p. This then immediately gives for the mass model, once again, $P(m) = \rho/(1+\rho)^{m+1}$.

Another exact result can be derived for the following asymmetric mass model. Instead of discrete mass, we now consider continuum masses at each site. The mass m_i at each site i evolves in discrete time according to the following stochastic equation,

$$m_i(t+1) = q_{i-1,i} m_{i-1}(t) + (1 - q_{i,i+1})\, m_i(t) \tag{18}$$

where the random variable $q_{i-1,i}$ represents the fraction of mass that breaks off from site $(i-1)$ and moves to site i. We assume that each of these fractions are independent and identically distributed in the interval $[0, 1]$ with some distribution function $\eta(q)$. We show in the Appendix that for the special case of uniform distribution, i.e., $\eta(q) = 1$ for all q in $[0, 1]$, the exact steady state distribution $P(m)$ is given by,

$$P(m) = \frac{4m}{\rho^2}\, e^{-2m/\rho} \tag{19}$$

where $\rho = \int_0^\infty mP(m)\, dm$ is the conserved mass density fixed by the initial condition. In the LG language, this would mean that if m_i is the distance between ith and $(i+1)$th particle, then the ith particle can jump to any distance between k and $k+dk$ to the right (without crossing the next particle on the right) with uniform rate $p(k \mid m_i)\, dk = (1/m_i)\, dk$. In order to verify the exact formula for $P(m)$ in Eq. (19) we performed numerical simulation in 1-d. In Fig. 7, we show for $\rho = 1$, the perfect agreement between the theoretical cumulative mass distribution, $F(m) = \int_0^m P(m')\, dm' = 1 - e^{-2m} - 2me^{-2m}$ and the numerically obtained points from the simulation. We note that a similar result was recently derived[34] in the context of the generalized Hammersley process.[35]

Thus in all these cases studied in this section, we find exponential decay of the mass distribution for large mass in the steady state. It would therefore seem that only for the special kernel, $p(k \mid m) = w\delta_{k,1} + \delta_{k,m}$, is

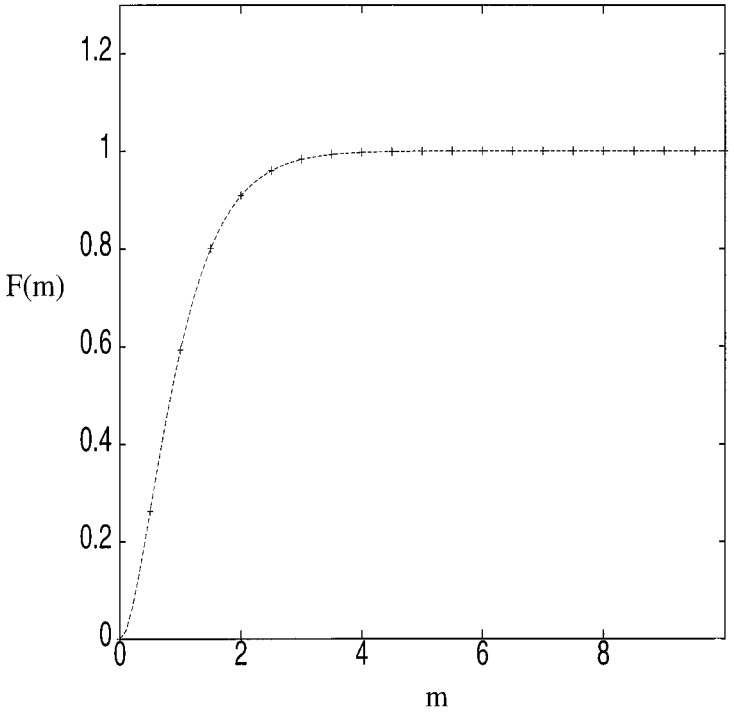

Fig. 7. The theoretical cumulative mass distribution function, $F(m) = 1 - e^{-2m} - 2me^{-2m}$ (continuous line) plotted against m along with the numerically obtained points from the simulation of the model in one dimension for mass density $\rho = 1$.

there a nontrivial phase transition from a phase where $P(m)$ decays exponentially to another where it has a power law decay in addition to an infinite aggregate. The presence of two delta function peaks in $p(k \mid m)$ seem to be crucially responsible for this phase transition. We believe that the phase transition will still persist if one allows for a nonzero width to the delta peaks at the two ends of the kernel near $k = 0$ and $k = m$ but making sure that the widths remain finite even as $m \to \infty$. This however needs further studies to be confirmed.

VIII. CONCLUSION

In this paper we have studied a lattice model of aggregation and dissociation where a mass from a site can either move as a whole to a neighbouring site with rate p_1 or can chip off a unit mass to a neighbour

with rate p_2. The hopped mass then aggregates instantaneously with the mass that is already present at the neighbour. The ratio of the rates, $w = p_2/p_1$ and the conserved mass density ρ are the only two parameters of the model. The steady state of the model undergoes a phase transition as the parameters (ρ, w) are varied. In the (ρ, w) plane there is a critical line that separates two phases: (i) the "Exponential" phase where the single site mass distribution $P(m)$ decays exponentially for large m and (ii) the "Aggregate" phase where $P(m)$ has a power law decay in addition to a delta function peak at $m = \infty$ signifying the presence of an infinite aggregate. On the critical line, the aggregate vanishes but $P(m) \sim m^{-\tau}$ retains the same power law tail. We have also studied how the universality class of this dynamical phase transition changes on applying a bias in a particular direction of the mass transport.

We have solved the model exactly within the mean field theory and presented numerical results for one dimension. Besides, by exploiting a mapping to a lattice gas model in 1-d, we have obtained the steady state distribution $P(m)$ exactly for small and large w. We have further mapped the lattice gas model to an interface model in $(1+1)$ dimension and studied the width of the interface that characterizes its fluctuations. We have calculated the roughness exponent χ and the dynamical exponent z analytically for small and large w both with and without bias. We have computed these exponents numerically at the critical point and shown that the two critical points (with and without bias) represent two new fixed points of interface dynamics in $(1+1)$ dimension.

We have also generalized our model to include arbitrary fragmentation kernels and obtained a few exact results for special choices of these kernels via mappings to other solvable statistical mechanics models studied in the recent past.

Our model obviously has some shortcomings as a model of realistic aggregation and fragmentation phenomena. For example, we have assumed that the rate of hopping of a mass as a whole is independent of the mass. In a realistic setting this is perhaps not a good approximation, and to model a specific system one needs to incorporate a mass-dependent hopping rate. This however has not been attempted in this paper, where our aim is to understand the mechanism of the dynamical phase transition induced by the basic microscopic processes of diffusion, aggregation and fragmentation within a simple setting.

However there remain many open questions even for this simple model. For example, in one dimension we were not able to compute analytically the various exponents at the critical point. Given that there has been recent progress in determining the exact steady states of a class of exclusion processes in one dimension via using a matrix product ansatz[33]

and coordinate Bethe ansatz,[36] it may be possible to obtain the exact steady states of our model in 1-d.

Another important open question that needs to be studied for both the symmetric and asymmetric models: What is the upper critical dimension d_c of these models beyond which the mean field exponents will be exact? In analogy to other diffusion limited models studied earlier,[37] one expects that in the symmetric case $d_c = 2$. This expectation is supported by the numerical fact that the exponent $\tau_s \approx 2.33$ in 1-d is already close to its mean field value 5/2. This conjecture however requires a proof.

The question of upper critical dimension is however puzzling for the asymmetric model where the numerical value of $\tau_{as} \approx 2.05$ (perhaps $\tau_{as} = 2$ with logarithmic corrections) is quite far from the mean field value 5/2. This indicates that the d_c (if there exists one) for the asymmetric case might even be bigger than 2, contrary to the naive expectation that the d_c of directed models is usually lower than that of undirected models. A numerical study of the asymmetric model in 2 dimensions may shed some light on this puzzle.

APPENDIX: EXACT RESULT FOR UNIFORM FRAGMENTATION KERNEL

In this appendix we solve exactly the steady state single site mass distribution function $P(m)$ for the model where the mass m_i at every site i evolves in discrete time according to the stochastic Eq. (18), where the fractions $q_{i,j}$ are independent and identically distributed random variables in $[0, 1]$ with distribution function $\eta(q)$. We note the formal similarity between Eq. (18) and the force balance equation in the q-model of Coppersmith *et al.*,[32]

$$W(i, D+1) = \sum_j q_{ji} W(j, D) + 1 \tag{20}$$

where $W(i, D)$ represents the net stress supported by a glass bead at a depth D in a cylinder and q_{ji} is the fraction of the stress transported from particle j at layer D to a particle i at layer $(D+1)$. The only difference between Eq. (18) and Eq. (20) is in the additional constant term 1 in Eq. (20) that is absent in Eq. (18). Nevertheless the same line of argument as in ref. 32 leads to an exact solution in our case also as we outline below.

We first consider the mean field theory where we neglect correlations between masses. For simplicity, we use the notations, $q_{i-1,i} = q_1$, $1 - q_{i,i+1} = q_2$, $m_{i-1} = m_1$ and $m_i = m_2$. Then the mass distribution satisfies

$$P(m, t+1) = \int_0^1 \int_0^1 dq_1\, dq_2\, \eta(q_1)\, \eta(1-q_2) \int_0^\infty \int_0^\infty dm_1\, dm_2 \times P(m_1, t)\, P(m_2, t)\, \delta(m - m_1 q_1 - m_2 q_2) \tag{21}$$

where we have used Eq. (18). In the limit $t \to \infty$ and for the uniform distribution $\eta(q) = 1$, the Laplace transform $\tilde{P}(s)$ of the distribution $P(m)$ satisfies the equation

$$\tilde{P}(s) = \left[\int_0^1 dq\, \tilde{P}(sq) \right]^2 \tag{22}$$

Defining $V(s) = \sqrt{\tilde{P}(s)}$ and $u = qs$, we get from Eq. (22),

$$sV(s) = \int_0^s du\, V^2(u) \tag{23}$$

Differentiation with respect to s yields

$$V(s) + s \frac{dV}{ds} = V^2(s) \tag{24}$$

which can be integrated to give

$$V(s) = \frac{1}{1 - Cs} \tag{25}$$

The constant C is determined from the mass conservation equation, $\int_0^\infty mP(m)\, dm = -d\tilde{P}(s)/ds|_{s=0} = \rho$ where ρ is the conserved mass density. Thus, $C = dV/ds|_{s=0} = -\rho/2$. Hence we get, $\tilde{P}(s) = 1/(1 + (\rho/2)\, s)^2$ and by inverse Laplace transform,

$$P(m) = \frac{4m}{\rho^2} e^{-2m/\rho} \tag{26}$$

This is the mean field result for $P(m)$. However in ref. 32, it was proved that for a uniform distribution $\eta(q) = 1$, the mean field stress distribution, where the stresses satisfy Eq. (20), is exact. The explicit algebraic proof in ref. 32 proceeded via constructing exact recursion relations for the joint probability distribution of the weights in row $(D+1)$ in terms of those for row D, and showing that the mean field factorization of these joint distributions are invariant under this recursion. The same line of proof can be adapted to show that the mean field result Eq. (26) is also exact for our

problem. We do not give details of the proof here as they can be found in ref. 32.

NOTE ADDED IN PROOF

As mentioned in the text, the mean-field phase diagram can be shown to be exact even though equations (1) and (2) make the approximation of ignoring correlations in the occupation of adjacent sites. In fact, more careful numerical analysis has shown that the mean-field answer for the single-point function $P(m)$ may also be exact, with the exponent value $\tau = 2.33$ reported in the text actually tending to the mean-field value $\tau = 2.5$ for large m.

ACKNOWLEDGMENTS

We thank D. Dhar and Rajesh R. for useful discussions and J. Krug for sending us a preprint of ref. 34.

REFERENCES

1. W. H. White, *J. Colloid Interface Sci.* **87**:204 (1982).
2. R. M. Ziff, *J. Stat. Phys.* **23**:241 (1980).
3. A. E. Scheidegger, *Bull. I.A.S.H.* **12**:15 (1967).
4. A. Maritan, A. Rinaldo, R. Rigon, A. Giacometti, and I. R. Iturbe, *Phys. Rev. E* **53**:1510 (1996); M. Cieplak, A. Giacometti, A. Maritan, A. Rinaldo, I. R. Iturbe, and J. R. Banavar, *J. Stat. Phys.* **91**:1 (1998).
5. S. K. Friedlander, *Smoke, Dust and Haze* (Wiley, Interscience, New York, 1977).
6. B. Lewis and J. C. Anderson, *Nucleation and Growth of Thin Films* (Academic Press, New York, 1978).
7. S. N. Majumdar, S. Krishnamurthy, and M. Barma, *Phys. Rev. Lett.* **81**:3691 (1998).
8. H. Takayasu, *Phys. Rev. Lett.* **63**:2563 (1989); H. Takayasu, I. Nishikawa, and H. Tasaki, *Phys. Rev. A* **37**:3110 (1988).
9. R. D. Vigil, R. M. Ziff, and B. Lu, *Phys. Rev. B* **38**:942 (1988).
10. P. L. Krapivsky and S. Redner, *Phys. Rev. E* **54**:3553 (1996).
11. G. Ananthakrishna, *Pramana* **12**:543 (1979).
12. X. Campi and H. Krivine, *Nucl. Phys. A* **620**:46 (1997).
13. J. Krug and P. A. Ferrari, *J. Phys. A* **29**:L446 (1996).
14. M. R. Evans, *J. Phys. A* **30**:5669 (1997).
15. G. Tripathy and M. Barma, *Phys. Rev. Lett.* **78**:3039 (1997); *Phys. Rev. E* **58**:1911 (1998).
16. M. Bengrine, A. Benyoussef, H. Ez-Zahraouy, and F. Mhirech, *Phys. Lett. A* **253**:135 (1999).
17. F. Ritort, *Phys. Rev. Lett.* **75**:1990 (1995).
18. O. J. O'Loan, M. R. Evans, and M. E. Cates, *Phys. Rev. E* **58**:1404 (1998).
19. Rajesh R., in preparation.
20. T. M. Ligget, *Interacting Particle Systems* (Springer-Verlag, New York, 1983).
21. J. Krug and H. Spohn, in *Solids Far From Equilibrium*, C. Godr'eche, ed. (Cambridge University Press, Cambridge, 1991); T. J. Halpin-Healy and Y. C. Zhang, *Phys. Rep.* **254**: 215 (1995).

22. S. F. Edwards and D. R. Wilkinson, *Proc. R. Soc. Lond. A* **381**:17 (1982).
23. J. M. Hammersley, in *Proceedings of the Fifth Berkeley Symposium on Mathematical Statistics and Probability*, L. M. le Cam and J. Neyman, eds. (University of California Press, Berkeley, 1967), Vol. III, p. 89.
24. M. Kardar, G. Parisi, and Y.-C. Zhang, *Phys. Rev. Lett.* **56**:889 (1986).
25. B. Schmittmann and R. K. P. Zia, *Statistical Mechanics of Driven Diffusive Systems*, Vol. 17, C. Domb and J. L. Lebowitz, eds. (Academic Press, London, 1995).
26. J. Krug, *Adv. Phys.* **46**:139 (1997).
27. S. N. Majumdar and D. A. Huse, *Phys. Rev. E* **52**:270 (1995).
28. A. J. Bray, *Adv. Phys.* **43**:357 (1994).
29. C. Sire and S. N. Majumdar, *Phys. Rev. E* **52**:244 (1995).
30. K. Klauck and A. Schadschneider, cond-mat/9812201.
31. R. Rajesh and D. Dhar, *Phys. Rev. Lett.* **81**:1646 (1998).
32. S. N. Coppersmith, C.-H. Liu, S. N. Majumdar, O. Narayan, and T. A. Witten, *Phys. Rev. E* **53**:4673 (1996).
33. B. Derrida and M. R. Evans, in *Nonequilibrium Statistical Mechanics in One Dimension*, V. Privman, ed. (Cambridge University Press, Cambridge, 1997).
34. J. Krug and J. Garcia, cond-mat/9909034.
35. P. A. Ferrari and L. R. G. Fontes, *El. J. Prob.* **3** (1998).
36. G. Schütz, *J. Stat. Phys.* **88**:427 (1997); V. Karimipour, cond-mat/9812403.
37. J. Cardy, *J. Phys. A Math. Gen.* **28**:L19 (1995), and references therein.